JOURNAL OF HORTICULTURE AND POSTHARVEST RESEARCH
2022, VOL. 5(1), 53-68

Journal of Horticulture and Postharvest Research

Journal homepage: www.jhpr.birjand.ac.ir

University of Birjand

Combination of numerical simulation and RSM to study the process factors on orange slices shrinkage

Seyad Jafar Hashemi[1] and Azadeh Ranjbar Nedamani[1*]

1, Biosystem Engineering Department, Sari Agricultural Sciences & Natural Resources University, POB: 578, Iran

ARTICLE INFO

Original Article

Article history:
Received 28 July 2021
Revised 29 October 2021
Accepted 16 November 2021
Available online 17 February 2022

Keywords:
CFD simulation
Fruit shrinkage
Modeling
Orange drying
Response surface methodology

DOI: 10.22077/jhpr.2021.4464.1225
P-ISSN: 2588-4883
E-ISSN: 2588-6169

***Corresponding author:**
Biosystem Engineering Department, Sari Agricultural Sciences & Natural Resources University, POB: 578, Iran.
Email: a.ranjbar@sanru.ac.ir

ABSTRACT

Purpose: Selecting the most effective factors and their combination during food processing, is critical to reduce the energy consumption, the time of process and also maintaining the final product properties. **Research method:** A definitive screen design of response surface methodology was designed by Design Expert software. Factors such as drying time (A: 20-60 °C), air velocity (B: 0.5-2.5 m/s), sample thickness (C: 3-7 mm), sample diameter (D: 4-6 cm), and drying time (E: 6000-10000s) were investigated. The treatments from response surface methodology were simulated in COMSOL software 5.3a. The simulated data such as moisture content, moisture ratio, central temperature of sample, and total shrinkage were used as surface responses in Design-Expert in order to find the effective process factors on orange drying. **Findings:** Orange drying simulations show the air temperature and its interaction with other process factors is effective on central temperature of samples. The moisture rate and moisture content depends on sample thickness and drying time, the shrinkage was a linear model as a function of thickness and process time. In orange samples, at thickness of 0.5mm, diameter of 4.8 cm, and drying time of 7379s the least shrinkage will occur according to prediction models. **Research limitations:** Calculating the experimental shrinkage, moisture ratio, and moisture rate were the research limitation for further simulation. **Originality/Value:** Combination the response surface methodology and COMSOL simulation in order to reducing the number of studied treatments. Finding the effective factors and their interactions and also the prediction model for final dried orange characteristics. Finding the shrinkage model of orange fruit with respect to the studied drying process factors.

INTRODUCTION

Food materials with high content of moisture such as fruits and vegetables are highly sensitive to deterioration. The deterioration of these food materials starts immediately after harvesting. To increase the shelf-life of such materials, their processing is necessary. Drying is the most common method for increasing the shelf-life of fruits and vegetables. The water activity reduction in dried food materials leads to reducing the reaction and microorganism's activity during storage. But the quality of dried food materials strongly depends on the drying process and storage condition (Adrover et al., 2019; Nguyen et al., 2018; Rojas et al., 2020). Some of these changes are shrinkage, texture rupturing, migration of solid materials onto the material surface, and reduction in rehydration rate (Kurozawa et al., 2012). Shrinkage is one of the most important changes during fruit and vegetable drying which can have a very important effect on the final product quality. Yuan et al. (2019) studied the drying of apple slices and numerically modeled the apple shrinkage. They used COMSOL software for simulation and found their mathematical models for heat and mass transfer can be used for simulation. Also, the found moisture stress has an important role in apple slices deformation during drying (Yuan et al., 2019). Curcio and Aversa (2014) formulated a theoretical model for predicting the convective behavior of a drier based on coupling the heat and mass transfer models by food structural mechanics models. They studied the effect of temperature distribution, moisture content, and strain, and stress on a cylindrical geometry of fresh potato shrinkage. They found their theoretical model is in good agreement with experimental data (Curcio & Aversa, 2014). Senadeera et al. (2020) studied the effect of temperature on drying characteristics (such as shrinkage) of persimmon in a hot air convective drier with a 2.3 m/s air velocity. They found a Quadratic model for evaluating the volumetric shrinkage based on moisture content (Senadeera et al., 2020). Onwude et al. (2018) investigate a new method to monitor and predict sweet potato shrinkage by computer vision, optical backscattering, and modeling with the artificial neural network. They found a linear relationship between moisture content and shrinkage. And the shrinkage is based on sample thickness, drying temperature, and time (Onwude et al., 2018). Nguyen et al. (2018) studied the impact of glass transition on non-cellular food systems shrinkage. They investigate the relationship between experimental and mathematical models of shrinkage. They found the glass transition alone is not a determinant factor for studying the porosity and volume changes during drying (Nguyen et al., 2018). Controlling the drying process parameters is critical during removing water from food material. The final food quality parameters such as color, texture, taste, and final industrial costs of the drying process are affected by selecting an effective combination of process factors. Thus selecting the most effective factors and their combination during food processing, is critical to reducing the energy consumption, the time of the process, and also maintaining the final product properties.

Since the drying process is a combination of heat and mass transfer, modeling and simulation of drying is a complex method to study the effect of process parameters on final product quality (Lin et al., 2009; Mutuli et al., 2020; Radojčin et al., 2021). In this study, we try to combine the response surface methodology (RSM) to investigate the most effective parameters on shrinkage of orange to find a model for further investigations. The aim of this study was a simulation and then selecting the most effective factors on orange slice shrinkage during the drying process.

Nomenclature			
A	area of the sample (m^2)	*Superscripts and subscripts*	
C_P	specific heat (J/kg K)	*a*	Air
D_{eff}	diffusion coefficient of orange (m^2/s)	*db*	dry basis
h	heat transfer coefficient (W/m^2 K)	*L*	fluid
k	thermal conductivity (W/m)	*s*	dry solid
MC	moisture content	*wb*	wet basis
S_R	shrinkage	*w*	water
T	temperature (K)	*p*	particle
t	time (s)		
Greek symbols			
ρ	density (kg/m^3)		
τ	tortuosity factor e		
ε	porosity		
θ	volume fraction		

MATERIALS AND METHODS

Here it is valuable to note that in this study, we used the experimental data for setting the simulation by COMSOL and after validation, we used the designed treatments by Design Expert. The further simulations were done at the basis of combination of different factors in designated treatments. Then we found the shrinkage or moisture content model and effective factors for each by simulated data.

Drying process

Oranges (*Citrus Sinensis* var. Marss) were harvested from trees at the ripening stage (Amol-Iran). The fruits were washed and sliced with 6 cm diameter and 3, 5, and 7 mm thickness. The diameter and thickness were measured by a Vernier caliper. Then the samples dried in a convective cabinet drier (BM120, 120L, Iran) at 60 ℃ and 0.5 m/s air velocity. The drier is equipped with an electric heater for heating the forced air. The circulation was done in the drier chamber with a centrifugal fan. The moisture content was monitored through a gravimetric method assumed the weight loss is dependent only on the moisture of the sample during the drying process. The weight changes were recorded every 40 min. The drying process stopped when the mass of samples has no longer changes. The mass changes were monitored with a digital electronic balance (Jadever-Sky600, Korea). The moisture content of samples was calculated as equation (1) (Golestani et al., 2013):

$$MC = \frac{M_0 - M_t}{M_0} \times 100 \qquad (1)$$

where the M_0 and M_t are the initial and final weight of samples, respectively. The M_0-M_t is the water mass retained in the sample.

The moisture ratio was calculated as equation (2) (Aral & Bese, 2016):

$$MR = \frac{M_t - M_e}{M_0 - M_e} \qquad (2)$$

where the M_t is moisture content of sample at any time of drying process (based on dry weight), the M_e is the equivalent moisture based on dry weight, and M_0 is the initial moisture content based on the dry weight.

The shrinkage during the drying process was calculated for diameter and thickness as equation (3) (Curcio and Aversa, 2014):

$$Shrinkage = \frac{X_0 - X_t}{X_f} \times 100 \qquad (3)$$

Where the X_0 is diameter/thickness at t = 0, the X_t is diameter/thickness at t, and X_f is diameter/thickness at the end of the drying process.

Response surface methodology

The before simulation, the RSM was used to evaluate the effect of drying process parameters on responses. By RSM, the simulation runs tend to reduce. Also, it will possible to study the different parameters in simulation. The DesignExpert v.11 software was used to find the treatments by a Screening factor design of RSM. Factors such as drying time (A: 20-60 ℃), air velocity (B: 0.5-2.5 m/s), sample thickness (C: 3-7 mm), sample diameter (D: 4-6 cm), and drying time (E: 6000-10000s) were investigated. The total 13 treatments are shown in Table 1. The results of these treatments were the weight, diameter, and thickness of samples (Ranjbar Nedamani & Hashemi, 2021).

After the simulation of all 13 treatments of Design Expert, the simulated results were collected and statistically analyzed by RSM (Aliakbarian et al., 2018; Atalar & Dervisoglu, 2015). The response variables were fitted to a second-order polynomial model (Equation (4)) which is generally able to describe the relationship between the responses and the independent variables (Sumic et al., 2016).

Where Y is the response, X_i and X_j are the independent variables affecting the response, and β_0, β_i, β_{ii} and β_{ij}, are the regression coefficients for the intercept, linear, quadratic, and interaction terms, respectively. To evaluate model adequacy and determine regression coefficients and statistical significance, the analysis of variance (ANOVA) was used. The Design-Expert v.11 was used for RSM statistical analysis. The results were statistically tested at the significance level of p= 0.05. The adequacy of the model was evaluated by the coefficient of determination (R^2), model p-value, and lack of fit testing (Aliakbarian et al., 2018; Lisboa et al., 2018; Majeed et al., 2016) and the coefficient of variation (CV). The CV is a measure of deviation from the mean values, which shows the reliability of the experiment. In general, CV<10% indicates better reliability (Islam Shishir et al., 2016).

Table 1. Definitive screen design in response surface methodology

Run number	Temperature (℃)	Inlet air velocity (m/s)	Sample thickness (mm)	Sample diameter (cm)	Drying time (s)
1	60	2.5	0.3	5	6000
2	40	2.5	0.3	4	10000
3	50	0.5	0.3	4	6000
4	50	2.5	0.7	6	10000
5	60	2.5	0.7	4	8000
6	60	0.5	0.5	4	10000
7	40	0.5	0.7	5	10000
8	40	2.5	0.5	6	6000
9	40	1.5	0.7	4	6000
10	60	0.5	0.7	6	6000
11	50	1.5	0.5	5	8000
12	60	1.5	0.3	6	10000
13	40	0.5	0.3	6	8000

$$Y = \beta_0 + \sum_{i=1}^{2} \beta_i X_i + \sum_{i=1}^{2} \beta_{ii} X_i^2 + \sum_{i<i=1}^{2} \beta_{ij} X_{ij} \quad (4)$$

Model definition and simulation with COMSOL

After finding the treatments in DesignExpert software, the simulation starts. At first, the experimental models of shrinkage, moisture content, and moisture ratio which were investigated by Excel and Sigmaplot, were used for simulation in COMSOL software. In COMSOL, the changes of mesh in the *x*, *y*, and *z*-direction were investigated for shrinkage in diameter and thickness of samples. The orange characteristics were as Table 2 (Hussain et al., 2021).

A 2D design was used to simulate the coupled laminar flow, heat transfer, and diluted species transfer (for mass transfer simulation). The calculations were based on the stationary and time-dependent study. The data saved at each 10s. For shrinkage study, the moving mesh module was used. The mesh changes in diameter and thickness were calculated from experimental functions extracted from lab data by SigmaPlot (Eq. 11-13). The mesh consists of 21616 elements by 0.836 qualities (Fig. 1). The COMSOL multiphysics 5.3a was used to solve four modules based on turbulent RANS k-ε. The processor was a surface desktop Intel® Core™ i5-4300U, 2.50 GHz, RAM 4 GB, and Windows 10 64-bit operating system. The relative tolerance was 0.01. The data were recorded every 1 min up to 10000 s.

Table 2. Orange characteristics for simulation.

Characteristics	Amount
Porosity	0.6
k	(W/m.K) 0.3860
c_p	(J/(kg.K) 3850
ρ	(kg/m^3) 960
α	(m^2/s) 3.05×10^{-5}

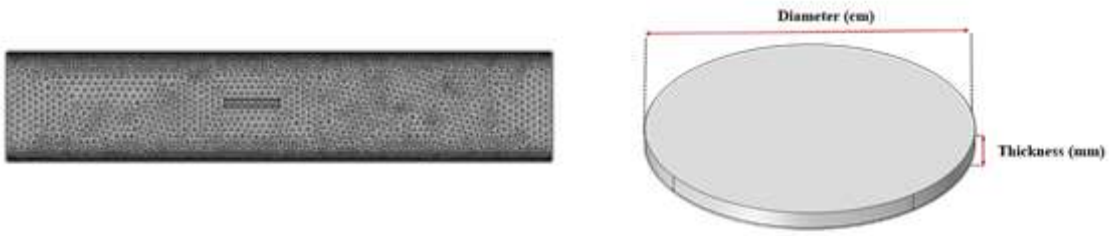

Fig. 1. An orange slice and the dryer meshing in COMSOL simulation

Governing equations

The heat transfer inside the porous media

The conductive heat transfer was governed through the Fourier equation.

$$\left(\rho C_p\right)_{eq}\frac{\partial T}{\partial t} = \nabla.\left(k_{eq}\nabla T\right) + Q \quad (5)$$

$$k_{eq} = \theta_p k_p + \left(1-\theta_p\right)k_L \quad (6)$$

$$\left(\rho C_p\right)_{eq} = \theta_p C_{p_p}\rho_p + \left(1-\theta_p\right)C_{p_L}\rho_L \quad (7)$$

Since there is no heat generation inside the samples, the Q assumed as null. The convective heat flux is calculated through q= h. (T_0 – T_i).

The mass transfer

The Fick's law used for mass transfer as bellow:

$$(\varepsilon)\frac{\partial y}{\partial x} + \left(C - \rho_p C_p\right)\frac{\partial y}{\partial x} = -\nabla.\left(D_{eff}.\nabla C\right) \quad (8)$$

$$D_{eff} = \varepsilon\tau D_f \quad (9)$$

$$\rho_p = \frac{\rho_b}{(1-\varepsilon)} \quad (10)$$

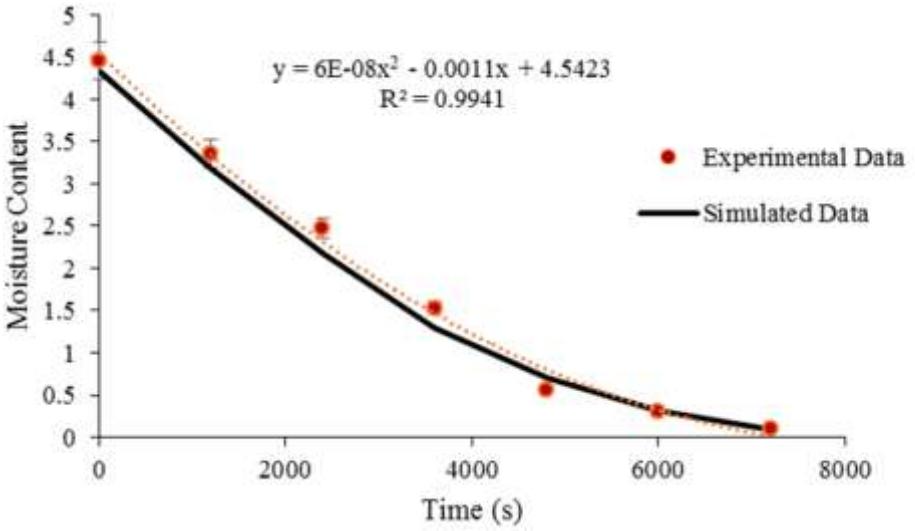

Fig. 2. Correlation between experimental and simulated moisture content

Moving mesh

After drying the samples, the experimental data were analyzed by Excel and SigmaPlot v.11 software to investigating the experimental functions and their regression coefficients. The functions of moisture content based on drying time, moisture ratio based on drying time, shrinkage based on moisture content, and shrinkage based on process time were experimentally obtained. Shrinkage was calculated for the diameter and thickness of the samples. The experimental thickness and diameter shrinkage models as a function of moisture content (*db*) were calculated as equitations 5 and 6, respectively:

$$Thickness\ shrinkage = 0.3012 \times (1 - \exp(-3934 \times MC) \qquad R^2 = 0.96 \quad (11)$$

$$Diameter\ shrinkage = 0.208 + (0.093 \times MC) - (5.19E - 005 \times MC^2) + 2.22E - 007 \times MC^3 \qquad R^2 = 0.91 \quad (12)$$

The shrinkage equations are then used as the moving mesh rate in COMSOL software for calculating the amount of shrinkage for thickness and diameter.

The bulk shrinkage was calculated as equation 4 (Lozano et al., 1980):

$$Bulk\ shrinkage = 0.11 \times MC + 0.17 \quad (13)$$

Statistical methods and model validation after simulation

The correlation between experimental data and simulated data of moisture content was investigated to study the correct simulation. The DesignExpert v.11 was used for statistical analysis of raw and simulated data. To find the significant factors and model adequacy, the ANOVA analysis based on a *P*-value of 0.05 was used. If the model or factor *P* value were lower than 0.05. The coefficient considered as significant.

RESULTS AND DISCUSSION

Validation the experimental data

The correlation between experimental and simulated moisture content for validation of simulation is shown in Figure 2. The figures show the moisture content has a logarithmic relationship with time. The high R^2 = 0.9941 shows the reliability of the computational fluid dynamics (CFD) simulation. The low error indicates the drying simulation based on experimental data can effectively predict the drying process of orange slices.

The experimental drying of orange samples

The dried samples are shown in Figure 3. Drying is a thermal process with heat and mass transfer during a determined time. The experimental data allowed achieving a detailed definition of influence the thickness of samples during the drying. During drying, the samples which are saturated with water lost their water gradually. Figures 4a and 4b, show the water evaporation from samples is not a linear model. The water evaporated at the first times of drying faster than the last times of drying process. The drying leads to evaporate the high free contents of water from samples at the first stages but with reducing the water concentration inside the samples, the later stages show a low steep moisture profile. Because of changes in the path of water molecules flow inside the sample stricter, the mobility of water reduces. This is attributed to the porosity and thus the diffusion coefficient changes (Adrover et al., 2019; Aprajeeta et al., 2015; Zecchi & Gerla, 2020). Also due to the torosity factor, the rate of drying at the last stage reduces. The torosity factor relates to the measure of the pass which the water molecules travelers to the surfaces of samples (Golestani et al., 2013; Hassini et al., 2007). At the first stage of drying, the water travels through a free diffusion but later, the movement is through the interstitial spaces which lead to a longer time to reach the water molecules to the surfaces. When the water moves toward the surface, the mechanical equilibrium and thus tissue structure of the sample will disturb due to the creation of some spaces with different transitions on both sides of them. This tension leads to a phenomenon named “shrinkage” which is an important factor for quality control of dried fruits. Figures 4c and 4d show the changes of sample dimension at diameter and thickness.

t=0 (min) t=40 (min) t=80 (min) t=120 (min) t=160 (min)

Fig. 3. The sample images during drying process for thickness 0.5 mm

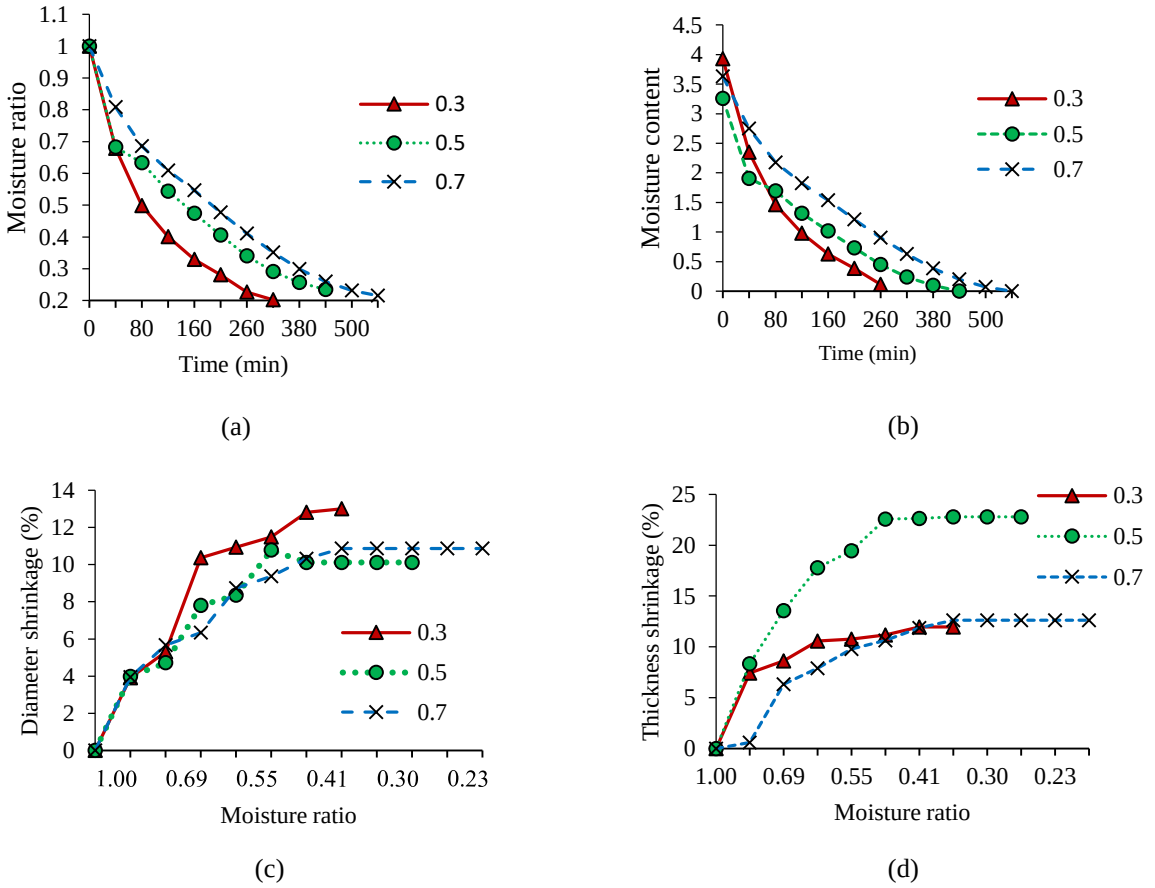

Fig. 4. Moisture ratio (a), Moisture content (b), Diameter (c) and thickness (d) shrinkage changes during orange drying at lab oven with 60°C and 0.5 m/s.

The experimental data of moisture content, moisture ratio, and diameter and thickness shrinkage of orange samples are shown in Figure 4. The sample with 0.3 mm thickness dried 300 min faster than the sample with 0.7 and 180 min faster than the sample with 0.5 mm thickness. The changes in moisture content and moisture ratio in orange samples are in agreement with other fruit drying studies (Brasiello et al., 2013; Castro et al., 2018; Hussain et al., 2021; Mutuli et al., 2020; Radojčin et al., 2021). Increasing the thickness of orange samples at a constant drying temperature leads to an increased process time. The data show the moisture content of samples depends on drying time and sample thickness. Also Figure 4 shows the samples with 0.5 mm thickness had the highest shrinkage than the two others, and in a moisture ratio of 0.48, its shrinkage reached a fixed amount of %11.922.56. While at the same moisture ratio, the samples with 0.3 and 0.5 mm thickness show the maximum amount of %10.6 shrinkages. Changes in the diameter of orange samples were different than the thickness changes. The highest change of diameter was %13.11 in samples with 0.3 mm thickness. While in 0.5 and 0.7 mm samples were %10.1 and %10.88, respectively. In the sample with a thickness of 0.5 mm, the percentage of shrinkage at thickness is much higher than the shrinkage at diameter. During drying, the pores of samples filled with water molecules, make the paths for water movement to the surface. This removal of water from pores disturbs the mechanical equilibrium of cells which leads to changes in sample structure. At the first stage of drying, this change is high, because the removal of water is high (Fig. 4c and 4d). The shrinkage is not linear with moisture ratio. At the first stages of shrinkage (both

at diameter and thickness shrinkage), the changes are faster with a rapid sleep but at the final stages, the structure changes are almost linear. Wang and Brennan (1995) explained the relation between the velocity of moisture removal and shrinkage is effective on the final shrinkage of samples. If the water removal is equal to shrinkage, the shrinkage will be uniform (Wang & Brennan, 1995). It is important during fruit drying. When the drying conditions are set well to make equilibrium for water removal velocity, then the shrinkage will be controllable and uniform. Thus knowing the parameter's effects on uniform water removal from samples is necessary. In this study, these experimental data were used to find the models of moisture content, moisture ratio, and shrinkage of orange samples. The experimental data were analyzed by SigmaPlot software and the equations for moisture content, moisture ratio, and diameter and thickness shrinkage of orange samples are shown in Table 3. The models with the highest regression parameters were selected. These models are then used for simulation in COMSOL software.

The simulated drying of orange samples

The simulation of shrinkage changes as a function of time during drying of the orange sample is shown in Figure 5. In the simulation, the air inlet was assumed at the left side of geometry. The shrinkage in thickness is higher at the side which the sample faces the air inlet. With proceeding the drying time, the changes in thickness and diameter proceed progressively. The shrinkage relates to water removal speed. When the inlet air is faced by the sample, the water removal is higher on that side. Thus the speed of shrinkage is higher than the other side of the sample. Similar results have been reported by (Aprajeeta et al., 2015; Curcio & Aversa, 2014). The side which is faced by inlet air reaches rapidly to a determined high temperature (Fig. 6).

This rapid increase in temperature at the initial stages of drying also is effective on water evaporation from samples and shrinkage. The temperature increasing in the sample, slows down when the process is proceeding. Then reaches a constant point to the final time of drying. Aprajeeta et al. (2015) explained this temperature reduction is due to dried layer thickness which heats transfers through it. If the drying process is internally controlled, the temperature effect becomes less significant and the dried layer thickness gradually increased, the temperature will be constant. Figure 6 also shows the simulated temperature, air velocity, and moisture content distribution of 13 RSM treatments. Since the air velocity, air temperature, and dimensions of samples are the most effective factors on shrinkage and final moisture content of samples (Ajani et al., 2019; Curcio & Aversa, 2014; Yadollahinia & Jahangiri, 2009; Ziaratban et al., 2017), the combination of these factors as RSM treatments make it possible to simulate the combination of drying process factors. It can be mentioned here that since the present simulation is based on a formulated set of factors, the proposed approach may be suitable for predicting the actual process performance. In this procedure, the RSM is useful for finding the statistical models which consider significant factors that affect each process's responses.

Table 3. Experimental models from experimental data of orange drying (*x* is processing time (s))

Thickness (mm)	Parameter	Model	R^2
0.3	Moisture rate	$y= 1.2089-0.2806x+0.0198x^2$	0.9791
	Moisture content	$y= 5.1594-1.5381x+0.1199x^2$	0.9833
	Thickness shrinkage	$y= -2.6866+4.7324x-0.3748x^2$	0.9092
	Diameter shrinkage	$y= -1.1826+1.0475x-0.0079x^2$	0.9844
0.5	Moisture rate	$y= 1.0773-0.1655x+0.0083x^2$	0.9653
	Moisture content	$y= 3.585-0.7045x+0.0353x^2$	0.9653
	Thickness shrinkage	$y= -5.6292+7.5247x-0.4801x^2$	0.9845
	Diameter shrinkage	$y= -2.7557+3.3753x-0.213x^2$	0.971
0.7	Moisture rate	$y= 1.0843-0.1354x+0.0053x^2$	0.992
	Moisture content	$y= 4.0228-0.6272x+0.0246x^2$	0.992
	Thickness shrinkage	$y= -3.8168+3.5453x-0.1855x^2$	0.9716
	Diameter shrinkage	$y= -1.7072+2.7057x-0.1412x^2$	0.9814

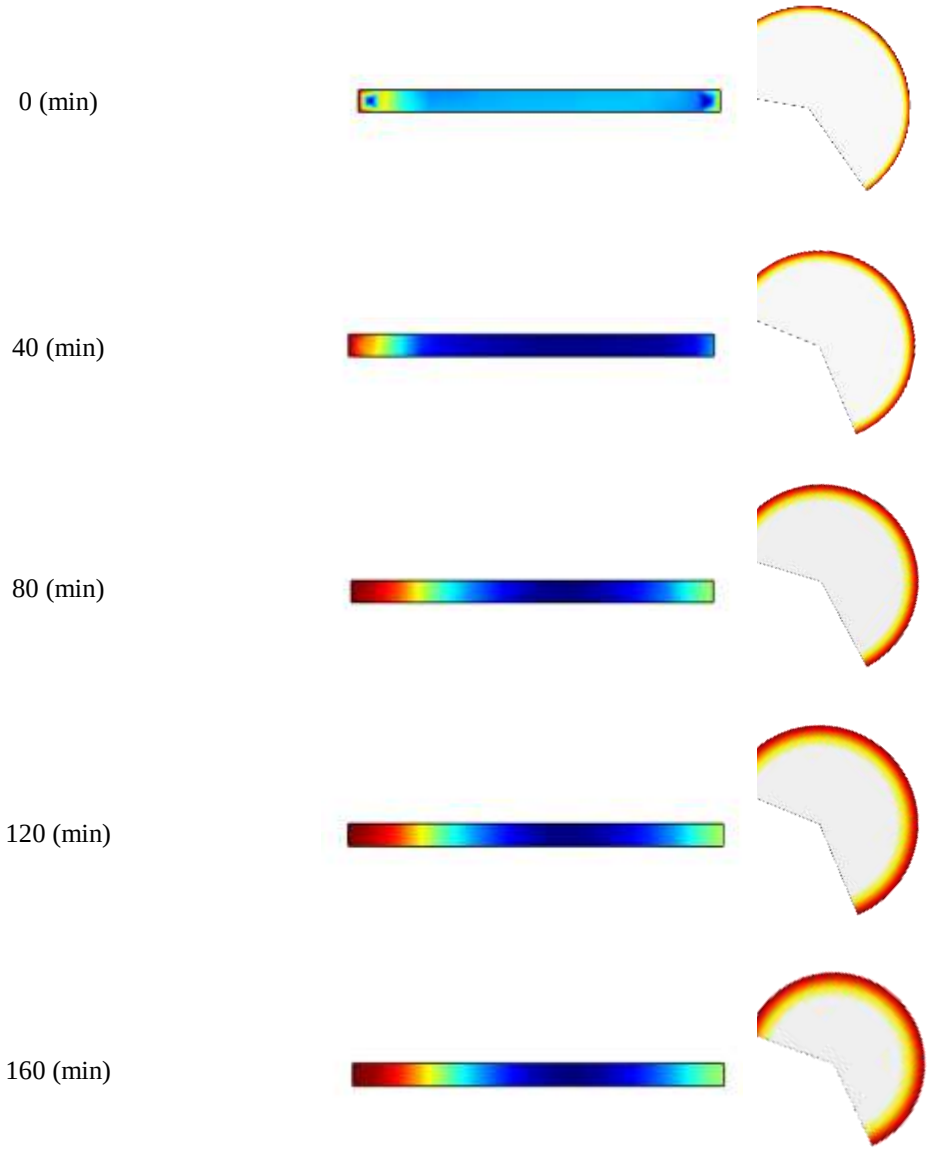

Fig. 5. The sample images during drying process for thickness 0.5 mm for shrinkage of thickness (a) and (b) diameter.

1

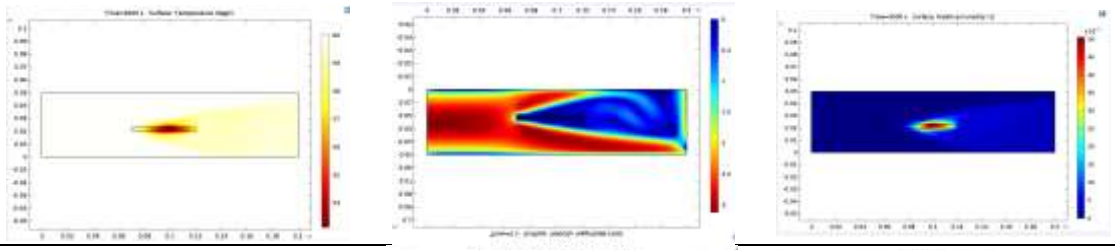

2

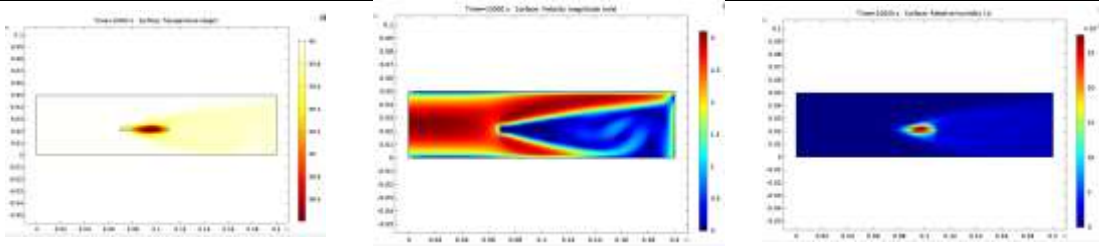

3

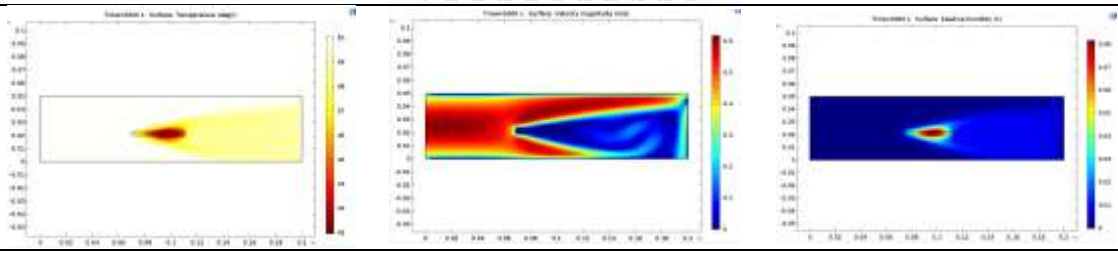

4

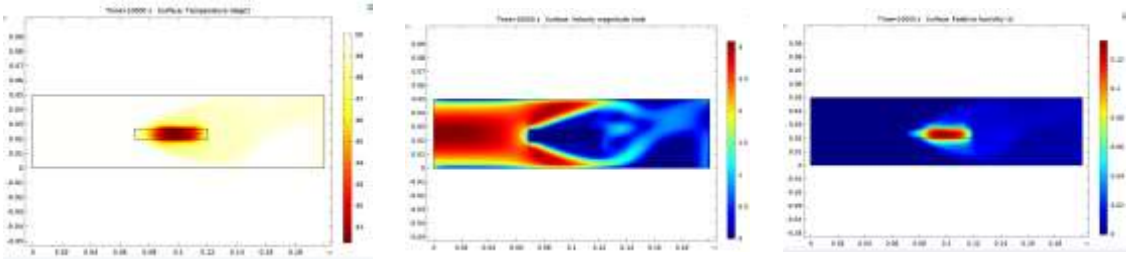

5

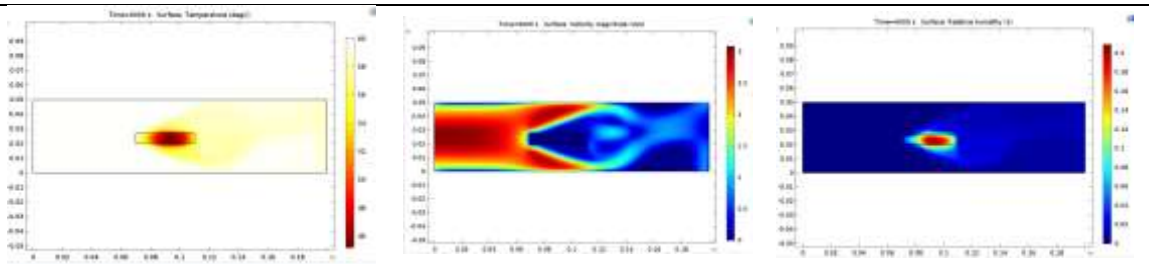

6

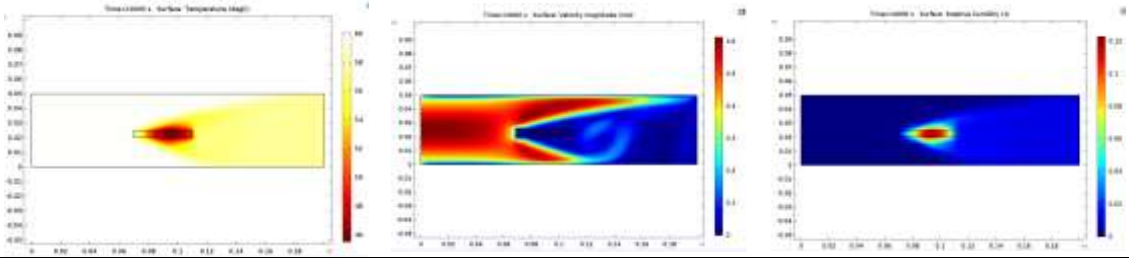

7

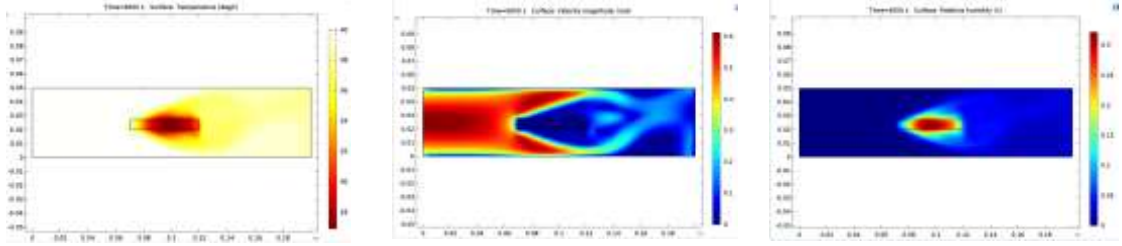

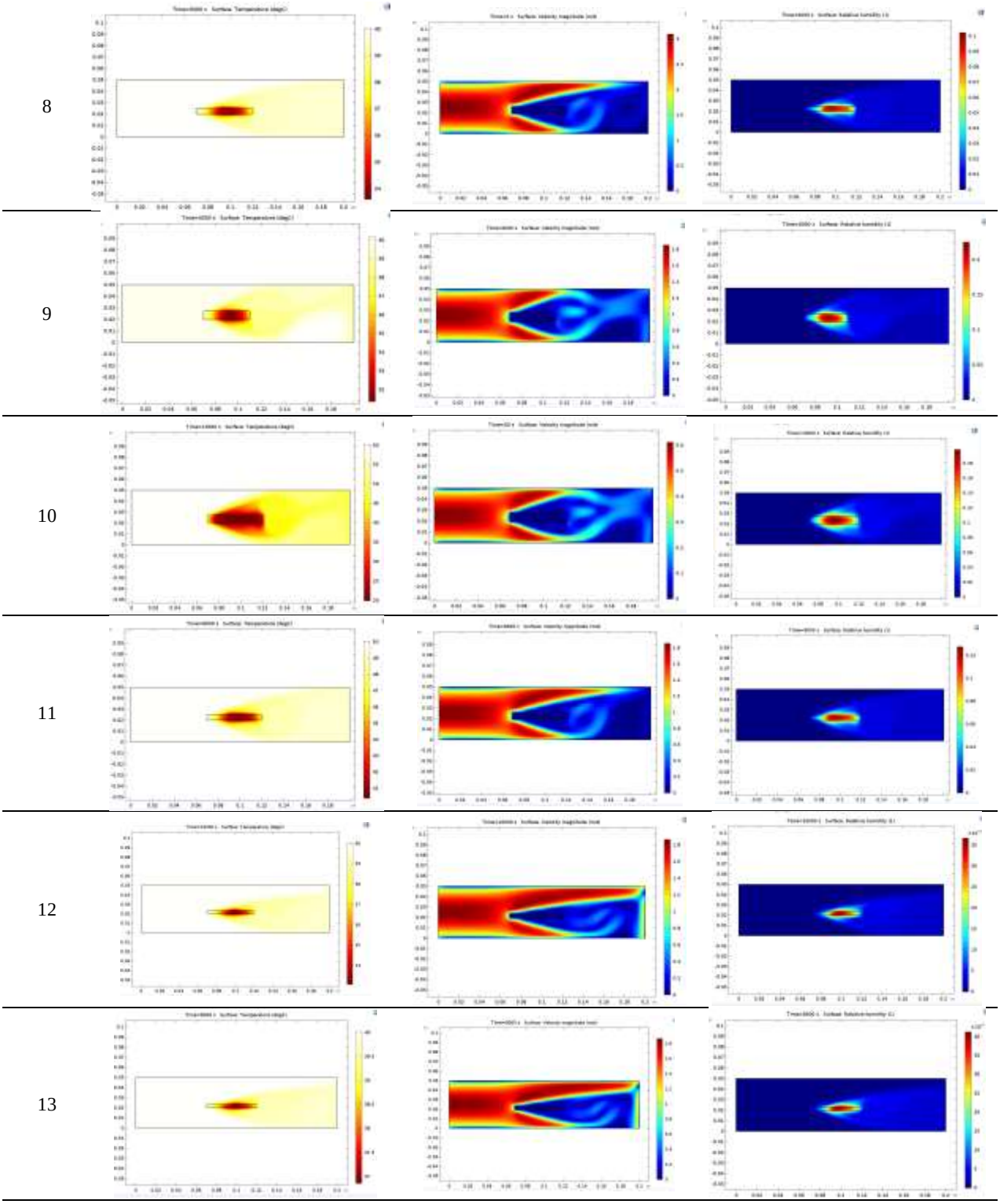

Fig. 6. Simulated temperature (a), air velocity (b), and moisture content distribution (c) of 13 RSM treat

Model fitting

The simulated data of orange drying in terms of internal temperature, moisture content, moisture ratio, and total shrinkage at the geometric point of simulated samples are listed in Table 4.

Table 4. ANOVA analysis of RSM for model parameters of orange sample

Source	Sum of squares	df	Mean square	F	P
		Central temperature			
Model	673.48	5	134.70	54.35	<0.0001*
A-Temperature	500.70	1	500.70	202.02	<0.0001*
B- Air velocity	34.71	1	34.71	14.00	0.0072*
C-Thickness	133.88	1	133.88	54.02	0.0002*
D-Diameter	0.0846	1	0.0846	0.0341	0.8586
E-Drying time	4.11	1	4.11	1.66	0.2388
Residuals	17.35	1	2.48		
Total	690.83	12			
		Moisture content			
Model	1.03	5	0.2061	6.21	0.0165*
A-Temperature	0.0758	1	0.0758	2.28	0.1745
B- Air velocity	0.1091	1	0.1091	3.29	0.1127
C-Thickness	0.3221	1	0.3221	9.70	0.0170*
D-Diameter	0.0881	1	0.0881	2.66	0.1472
E-Drying time	0.4353	1	0.4353	13.12	0.0085*
Residuals	0.2323	1	0.0332		
Total	1.26	12			
		Moisture ratio			
Model	0.0679	5	0.0136	7.51	0.0098*
A-Temperature	0.0037	1	0.0037	2.07	0.1934
B- Air velocity	0.0059	1	0.0059	3.27	0.1136
C-Thickness	0.0282	1	0.0282	15.59	0.0055*
D-Diameter	0.0039	1	0.0039	2.14	0.1873
E-Drying time	0.0262	1	0.0262	14.50	0.0066*
Residuals	0.0127	1	0,.0018		
Total	0.0806	12			
		Total shrinkage			
Model	1756.05	5	159.64	1596.41	0.0195*
A-Temperature	21.03	1	21.03	210.25	0.0435*
B- Air velocity	10.20	1	10.20	102.01	0.0628
C-Thickness	2.30	1	2.30	23.04	0.1308
D-Diameter	0.0490	1	0.0490	0.4900	0.6112
E-Drying time	30.28	1	30.28	302.76	0.0365*
AB	32.05	1	32.05	320.50	0.0355*
AC	128.20	1	128.20	1281.99	0.0187*
AD	509.04	1	509.04	5090.41	0.0089*
AE	401.46	1	401.46	4014.62	0.0100*
BC	536.91	1	436.91	4369.07	0.0096*
A^2	490.08	1	490.08	4900.79	0.0091*
Residuals	0.1	1	0.1		
Total	1756.15	12			

The sign * show the independent factor has significant effect on the response at $p<0.05$.

These simulated values were used as raw data for the RSM program to generate the most fitted predictive model and statistical analysis at $P< 0.05$. Responses were associated with independent variables and higher R^2, and the following models based on coded factors were determined using equation (4):

$$T = 40.77 + 7.08A + 1.86B - 3.66C \quad R^2 = 0.9992 \quad (14)$$

$$\ln(MC) = 0.3607 + 0.1795C - 0.2086E \quad R^2 = 0.8160 \quad (15)$$

$$MR = 0.5184 + 0.2655C - 0.000026E \quad R^2 = 0.8429 \quad (16)$$

$$Total\ shrinkage = 1.45A + 1.74E + 4.78AB + 9.74AC = 10.09AD + 21.58AE - 25.60BC - 27.65A^2 \quad R^2 = 0.999 \quad (17)$$

According to equation 14, the temperature of the sample depends on the temperature of inlet air, the velocity of inlet air, and the thickness of the sample. With respect to Equations 15 and 16, the thickness of samples and drying time are the only factors that had a significant role in moisture content and moisture rate.

While equation 17 indicates that the inlet air temperature and velocity, the sample thickness and drying time had a significant effect on final product temperature. When these factors are controlled during drying time, the water temperature distribution inside the sample, the water removal, and finally the shrinkage of the final sample will be uniform. This is necessary for manufacture the dried foods with a uniform final structure, especially in dried fruit slices.

CONCLUSION

The results show to reducing the shrinkage and drying process time, the inlet air temperature and sample thickness had a significant role. Also, when the shrinkage of the sample progresses during drying, the changes inside the sample reduces. At the first stages of drying, the temperature inside the sample reaches its higher amount but then stays constant to the final stage of drying. This is important from the heat and mass transfer viewpoint. These results show studying the experimental data with CFD methods, and a combination of these methods with RSM can help to find the models that have high accuracy and can predict the drying process more effectively.

Conflict of interest

There is no conflict of interest by the authors.

REFERENCES

Adrover, A., Brasiello, A., & Ponso, G. (2019). A moving boundary model for food isothermal drying and shrinkage: A shortcut numerical method for estimating the shrinkage factor. *Journal of Food Engineering, 244*, 212-219. https://doi.org/10.1016/j.jfoodeng.2018.09.030

Ajani, C., Curcio, S., Dejchanchaiwong, R., & Tekasakul, P. (2019). Influence of shrinkage during natural rubber sheet drying: Numerical modeling of heat and mass transfer. *Applied Thermal Engineering, 149*, 798-806. https://doi.org/10.1016/j.applthermaleng.2018.12.054

Aliakbarian, B., Sampaio, F. C., de Faria, J. T., Pitangui, C. G., Lovaglio, F., Casazza, A. A., . . . Perego, P. (2018). Optimization of spray drying microencapsulation of olive pomace polyphenols using Response Surface Methodology and Artificial Neural Network. *LWT*, *93*, 220-228. https://doi.org/10.1016/j.lwt.2018.03.048

Aprajeeta, J., Gopirajah, R., & Anandharamakrishnan, C. (2015). Shrinkage and porosity effects on heat and mass transfer during potato drying. *Journal of Food Engineering*, *144*, 119-128. https://doi.org/10.1016/j.jfoodeng.2014.08.004

Aral, S., & Bese, A. V. (2016). Convective drying of hawthorn fruit (Crataegus spp.): Effect of experimental parameters on drying kinetics, color, shrinkage, and rehydration capacity. *Food Chemistry*, *210*, 577-584. https://doi.org/10.1016/j.foodchem.2016.04.128

Atalar, I., & Dervisoglu, M. (2015). Optimization of spray drying process parameters for kefir powder using response surface methodology. *LWT - Food Science and Technology*, *60*(2, Part 1), 751-757. https://doi.org/10.1016/j.lwt.2014.10.023

Brasiello, A., Adiletta, G., Russo, P., Crescitelli, S., Albanese, D., & Di Matteo, M. (2013). Mathematical modeling of eggplant drying: Shrinkage effect. *Journal of Food Engineering*, *114*(1), 99-105. https://doi.org/10.1016/j.jfoodeng.2012.07.031

Castro, A. M., Mayorga, E. Y., & Moreno, F. L. (2018). Mathematical modelling of convective drying of fruits: A review. *Journal of Food Engineering*, *223*, 152-167. https://doi.org/10.1016/j.jfoodeng.2017.12.012

Curcio, S., & Aversa, M. (2014). Influence of shrinkage on convective drying of fresh vegetables: A theoretical model. *Journal of Food Engineering*, *123*, 36-49. https://doi.org/10.1016/j.jfoodeng.2013.09.014

Golestani, R., Raisi, A., & Aroujalian, A. (2013). Mathematical Modeling on Air Drying of Apples Considering Shrinkage and Variable Diffusion Coefficient. *Drying Technology*, *31*(1), 40-51. https://doi.org/10.1080/07373937.2012.714826

Hassini, L., Azzouz, S., Peczalski, R., & Belghith, A. (2007). Estimation of potato moisture diffusivity from convective drying kinetics with correction for shrinkage. *Journal of Food Engineering*, *79*(1), 47-56. https://doi.org/10.1016/j.jfoodeng.2006.01.025

Hussain, T., Kamal, M. A., & Hafiz, A. (2021). Comparative analysis of apple and orange during forced convection cooling: experimental and numerical investigation [J]. *AIMS Energy*, *9*(2), 193-212. https://doi.org/10.3934/energy.2021011

Islam Shishir, M. R., Taip, F. S., Aziz, N. A., Talib, R. A., & Hossain Sarker, M. S. (2016). Optimization of spray drying parameters for pink guava powder using RSM. *Food Science and Biotechnoly*, *25*(2), 461-468. https://doi.org/10.1007/s10068-016-0064-0

Kurozawa, L. E., Hubinger, M. D., & Park, K. J. (2012). Glass transition phenomenon on shrinkage of papaya during convective drying. *Journal of Food Engineering*, *108*(1), 43-50. https://doi.org/10.1016/j.jfoodeng.2011.07.033

Lin, Y., Li, S., Zhu, Y., Bingol, G., Pan, Z., & McHugh, T. H. (2009). Heat and mass transfer modeling of apple slices under simultaneous infrared dry blanching and dehydration process. *Drying Technology*, *27*(10), 1051-1059. https://doi.org/10.1080/07373930903218446

Lisboa, H. M., Duarte, M. E., & Cavalcanti-Mata, M. E. (2018). Modeling of food drying processes in industrial spray dryers. *Food and Bioproducts Processing*, *107*, 49-60. https://doi.org/10.1016/j.fbp.2017.09.006

Lozano, J., Rotstein, E., & Urbicain, M. (1980). Total porosity and open-pore porosity in the drying of fruits. *Journal of Food Science*, *45*(5), 1403-1407. https://doi.org/10.1111/j.1365-2621.1980.tb06564.x

Majeed, M., Hussain, A. I., Chatha, S. A., Khosa, M. K., Kamal, G. M., Kamal, M. A., . . . Liu, M. (2016). Optimization protocol for the extraction of antioxidant components from Origanum vulgare leaves using response surface methodology. *Saudi Journal of Biological Sciences*, *23*(3), 389-396. https://doi.org/10.1016/j.sjbs.2015.04.010

Mutuli, G. P., Gitau, A. N., & Mbuge, D. O. (2020). Convective Drying Modeling Approaches: a Review for Herbs, Vegetables, and Fruits. *Journal of Biosystems Engineering*, 1-16. https://doi.org/10.1007/s42853-020-00056-9

Nguyen, T. K., Khalloufi, S., Mondor, M., & Ratti, C. (2018). Shrinkage and porosity evolution during air-drying of non-cellular food systems: Experimental data versus mathematical modelling. *Food Research International*, *103*, 215-225. https://doi.org/10.1016/j.foodres.2017.10.013

Onwude, D. I., Hashim, N., Abdan, K., Janius, R., & Chen, G. (2018). The potential of computer vision, optical backscattering parameters and artificial neural network modelling in monitoring the shrinkage of sweet potato (*Ipomoea batatas* L.) during drying. *Journal of Science of Food and Agriculture*, *98*(4), 1310-1324. https://doi.org/10.1002/jsfa.8595

Radojčin, M., Pavkov, I., Bursać Kovačević, D., Putnik, P., Wiktor, A., Stamenković, Z., . . . Gere, A. (2021a). Effect of selected drying methods and emerging drying intensification technologies on the quality of dried fruit: A Review. *Processes*, *9*(1), 132. https://doi.org/10.3390/pr9010132

Ranjbar Nedamani, A., & Hashemi, S. J. (2021). RSM-CFD modeling for optimizing the apricot water evaporation. *Journal of Food and Bioprocess Engineering*, 4 (2), 112-119. https://doi.org/10.22059/jfabe.2021.320809.1088

Rojas, M. L., Augusto, P. E. D., & Cárcel, J. A. (2020). Ethanol pre-treatment to ultrasound-assisted convective drying of apple. *Innovative Food Science & Emerging Technologies*, *61*. https://doi.org/10.1016/j.ifset.2020.102328

Senadeera, W., Adiletta, G., Onal, B., Di Matteo, M., & Russo, P. (2020). Influence of different hot air drying temperatures on drying kinetics, shrinkage, and colour of persimmon slices. *Foods*, *9*(1). https://doi.org/10.3390/foods9010101

Sumic, Z., Vakula, A., Tepic, A., Cakarevic, J., Vitas, J., & Pavlic, B. (2016). Modeling and optimization of red currants vacuum drying process by response surface methodology (RSM). *Food Chemistry*, *203*, 465-475. https://doi.org/10.1016/j.foodchem.2016.02.109

Wang, N., & Brennan, J. (1995). Changes in structure, density and porosity of potato during dehydration. *Journal of Food Engineering*, *24*(1), 61-76. https://doi.org/10.1016/0260-8774(94)P1608-Z

Yadollahinia, A., & Jahangiri, M. (2009). Shrinkage of potato slice during drying. *Journal of Food Engineering*, *94*(1), 52-58. https://doi.org/10.1016/j.jfoodeng.2009.02.028

Yuan, Y., Tan, L., Xu, Y., Yuan, Y., & Dong, J. (2019). Numerical and experimental study on drying shrinkage-deformation of apple slices during process of heat-mass transfer. *International Journal of Thermal Sciences*, *136*, 539-548. https://doi.org/10.1016/j.ijthermalsci.2018.10.042

Zecchi, B., & Gerla, P. (2020). Effective diffusion coefficients and mass flux ratio during osmotic dehydration considering real shape and shrinkage. *Journal of Food Engineering*, *274*, 109821. https://doi.org/10.1016/j.jfoodeng.2019.109821

Ziaratban, A., Azadbakht, M., & Ghasemnezhad, A. (2017). Modeling of volume and surface area of apple from their geometric characteristics and artificial neural network. *International Journal of Food Properties*, *20*(4), 762-768. https://doi.org/10.1080/10942912.2016.1180533